REPORT DOCUMENTATION PAGE

Form Approved
OMB No. 0704-0188

1. REPORT DATE *(DD-MM-YYYY)*	2. REPORT TYPE	3. DATES COVERED *(From - To)*
30-09-2017	Performance/Technical Report (Quarterly)	07/01/2017 – 09/30/2017

4. TITLE AND SUBTITLE
A Hybrid Approach to Composite Damage and Failure Analysis Combining Synergistic Damage Mechanics and Peridynamics

5a. CONTRACT NUMBER

5b. GRANT NUMBER
N00014-16-1-2173

5c. PROGRAM ELEMENT NUMBER

6. AUTHOR(S)
Dr. Ramesh Talreja

5d. PROJECT NUMBER

5e. TASK NUMBER

5f. WORK UNIT NUMBER

7. PERFORMING ORGANIZATION NAME(S) AND ADDRESS(ES)

Texas A&M Engineering Experiment Station (TEES)
400 Harvey Mitchell Parkway, Suite 300
College Station, Texas 77845

8. PERFORMING ORGANIZATION REPORT NUMBER
M1601473 / 505170-00001/2

9. SPONSORING / MONITORING AGENCY NAME(S) AND ADDRESS(ES)
Office of Naval Research
875 N. Randolph Street, Suite 1425
Arlington, VA 22203-1995

10. SPONSOR/MONITOR'S ACRONYM(S)
ONR

11. SPONSOR/MONITOR'S REPORT NUMBER(S)

12. DISTRIBUTION / AVAILABILITY STATEMENT
unlimited

13. SUPPLEMENTARY NOTES

14. ABSTRACT

The work performed in the reporting period has been focused on completion of Task 1.2, and a part of Task 1.3 and Task 2.2, 2.4 described in the project proposal. The activities related to Task 1.2 concern growth and instability of initiated cracks in the environment of the disordered fiber distribution, and Task 1.3 evaluates the effect of these cracks on the response of the composite to imposed impulses. The activities related to Task 2 cover the new peridynamic model for multi-phase composites which can introduce the presence of pores and manufacturing defects in the intermediately-homogenized model of fiber-reinforced composites.

15. SUBJECT TERMS
Computational micromechanics; Cavitation induced cracking; Peridynamics; Porous media

16. SECURITY CLASSIFICATION OF:			17. LIMITATION OF ABSTRACT	18. NUMBER OF PAGES	19a. NAME OF RESPONSIBLE PERSON
a. REPORT	b. ABSTRACT	c. THIS PAGE			William Nickerson
U	U	U	SAR	7	19b. TELEPHONE NUMBER *(include area code)* 703-696-8485

Quarterly Progress Report, July 1 – September 30, 2017

A Hybrid Approach to Composite Damage and Failure Analysis Combining Synergistic Damage Mechanics and Peridynamics

Award Number N00014-16-1-2173

DOD – NAVY – Office of Naval Research

PI: Ramesh Talreja
Co-PI: Florin Bobaru

Executive Summary

The work performed in the reporting period has been focused on completion of Task 1.2, and a part of Task 1.3 and Task 2.2, 2.4 described in the project proposal. The activities related to Task 1.2 concern growth and instability of initiated cracks in the environment of the disordered fiber distribution, and Task 1.3 evaluates the effect of these cracks on the response of the composite to imposed impulses. The activities related to Task 2 cover the new peridynamic model for multi-phase composites which can introduce the presence of pores and manufacturing defects in the intermediately-homogenized model of fiber-reinforced composites.

Tasks 1.2 and 1.3 Modeling of RVE for Response of Composite with Damage

For the study of damage initiation and crack formation in composite materials that are processed by resin infusion in fiber bundles, a methodology for RVE generation was developed. The RVE generated comprises of the manufacturing induced features such a random distribution of fibers and the presence of matrix voids, which cause stress enhancement and hence damage initiation. In a systematic study, it was observed that RVE so generated had edge effects, leading to erroneous results close to the boundary in all imposed loading conditions. In order to mitigate this effect, the method of embedding the RVE in a composite cell was adopted. The typical model assembly is as shown in the Figure 1. In the figure shown, the boundary is 0.25R away from the outer edge of the RVE, where R is the radius of the circle of matrix enclosing the outermost fiber in the RVE. This RVE would still be giving erroneous results close to the boundary. However, since the fiber clustering occurs away from the outer regions of the RVE, the stress fields of interest are expected to be accurately calculated.

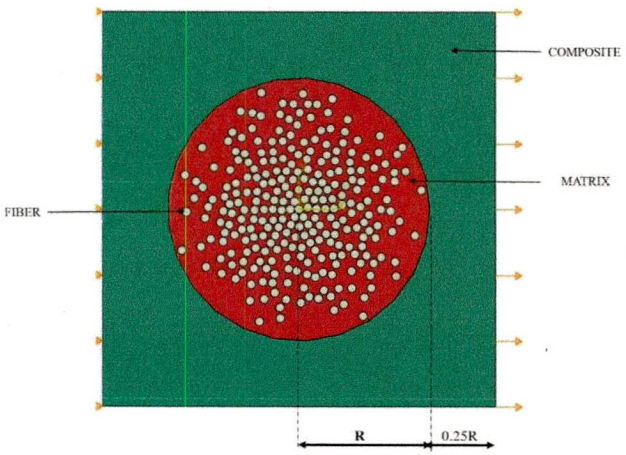

Figure 1: Model Assembly of the RVE

The size of the embedding composite region was determined based on Hill's criterion, which states that uniform displacement at the boundary should yield uniform traction at the same boundary. Based on this, different sizes of the embedding composite layers were chosen and traction at the boundary where displacement was applied was monitored. The results are as shown in Figure 2. The studies show that the size of the model assembly, L, was required to be 40R in order to overcome the effect of edge on the RVE.

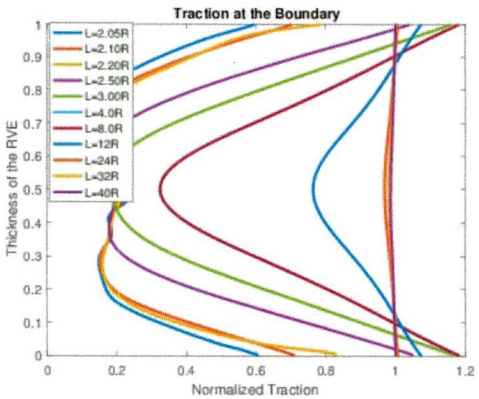

Figure 2: Traction at the boundary for varying thickness of the embedding composite layer

This would make the model assemble very large and the cost of computation would increase exponentially with the increase in number of elements. Thus, it was required to reduce the size of the model assembly at the same time remove the edge effects. Hence, we implemented the concept of effective embedding cell, as follows.

Effective Embedded Cell Model

Figure 3 represents the schematic of the model assembly where the RVE is embedded in an effective composite material. The mechanical behavior of the effective composite

material was determined iteratively. The dimension of the effective composite was assumed such that L/ R=5.

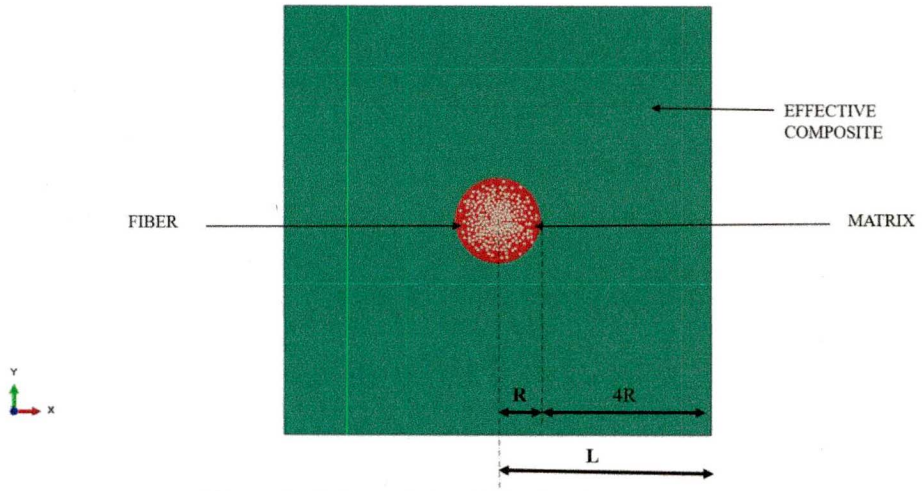

Figure 3: Schematic for Effective Embedded Cell

Iterative Procedure:
Under transverse displacement at the boundary of the model assembly, the response of the inner RVE was monitored. The hydrostatic stress was plotted with respect to the hydrostatic strain for the RVE. Figure 4 shows convergence of the stress for various iterations. An initially assumed composite property is modified after each iteration until the convergence of the behavior of the RVE is obtained.

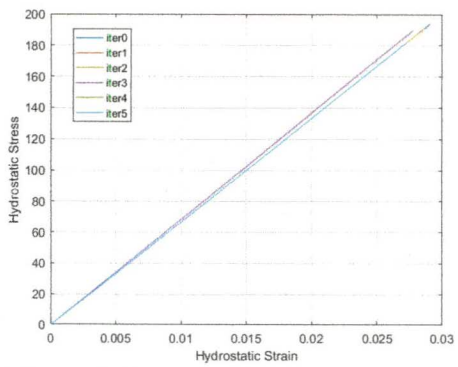

Figure 4 : Hydrostatic Stress-Strain curves for different iterations.

Figure 5 shows the convergence of the dilatation strain energy density for the iterations. It was observed that after the first few iterations the hydrostatic stress and strain curves converged and the effective properties of the composite was taken for the embedding cell for the damage initiation studies. This analysis was carried out for all realizations of varying radial mobility. The Table below shows the comparison of the dilatational strain energy density values for different realizations when embedded in different materials.

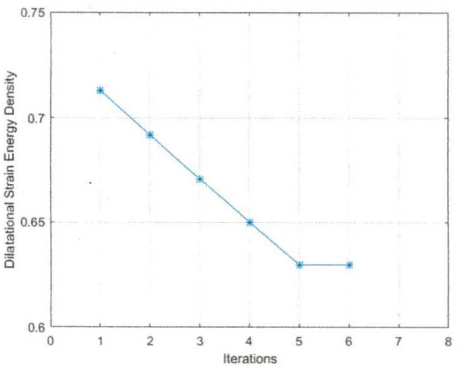

Figure 5: Dilatational Strain Energy Density for different iterations

Realization	RVE Embedded in Matrix	RVE Embedded in Composite	RVE embedded in Effective Composite
1	0.063	0.950	0.630(6 iteration)
2	0.057	0.870	0.540(5 iterations)
3	0.054	0.834	0.532(6 iteration)
4	0.066	0.99	0.643(6 iterations)

The ongoing research will focus on the analysis of response determined on the basis of the RVE developed taking different extent of the damage incurred within the RVE.

Tasks 2.2 and 2.4 Modeling of material interfaces and damage initiation and failure in a porous brittle sample.

Failure in composite materials starts at defects, pores, microcracks, or interfaces. To better understand the behavior of a peridynamic model for a two-phase composite at a material interface, we have conducted convergence studies in terms of strains across a material interface for a two-phase material sample under tensile loading transverse to the material interface. When the horizon size decreases, the jump discontinuity in horizontal strain across the interface, present in the exact solution of the local model, is well approximated by the peridynamic model (see Figure 6).

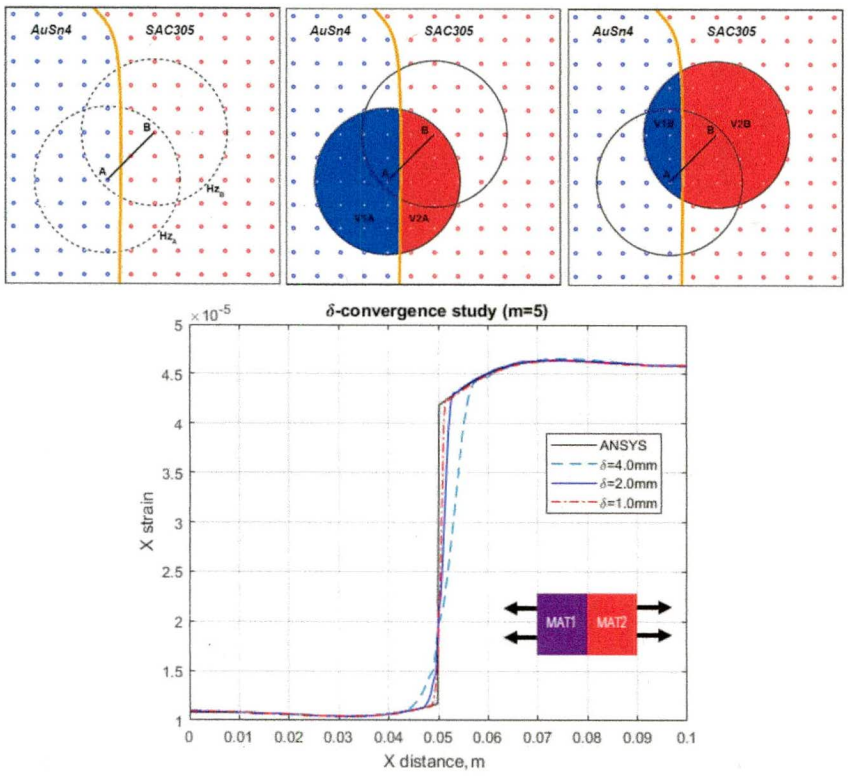

Figure 6: Top: scheme for computing the bond properties for interface bonds (bonds that cross a material interface) in the peridynamic model for a two-phase composite. Bottom: Convergence results for horizontal strain across a material interface using the "volumetric-averaging" shown above.

Continuing our work on the effect defects (like pores) have on the initiation and evolution of damage and failure, we performed a detailed peridynamic analysis of failure in a porous sandstone for which there are experimental results based on acoustic emissions that show the location of fracture events in the initial stages of failure in a three-point bending test with an asymmetric notch. In Figure 7, we overall the peridynamic results (blue-green-yellow-red colors), with the experimentally obtained acoustic emission data (orange squares), and with computational results obtained with a modified DEM model from Lin Q, Fakhimi A, Haggerty M, Labuz J. Initiation of tensile and mixed-mode fracture in sandstone. *Int J Rock Mech Min Sci.* 2009;46(3):489-497.

The results in Figs. 7 and 8 show several points:

(a) The peridynamic solution performs better than the DEM model as it captures the initiation of the failure zone at the notch near the right-corner of the tip of the notch. The DEM model shows the crack starting on the left corner of the notch tip. The acoustic emissions are clustered near the right-corner of the notch tip.

(b) The PD solution and the DEM solution separate past the middle point of the crack front. Experimental results from the reference cited above were not

reported in terms of the final failure of the sample. However, the significant difference between the failure zone near the bottom center of the sample between the DEM and the experiments, lead us to believe that the PD result is the accurate solution and not the DEM result.

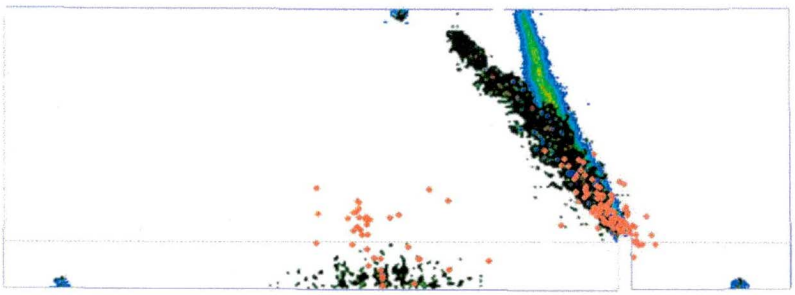

Figure 7: Failure in porous sandstone from three-point bending of a notched sample. Orange data is from acoustic emission measurements, black dots from a discrete element computation performed in the reference cited above, and the blue-green-yelow data is from the peridynamic model of a material with initial defects (pores).

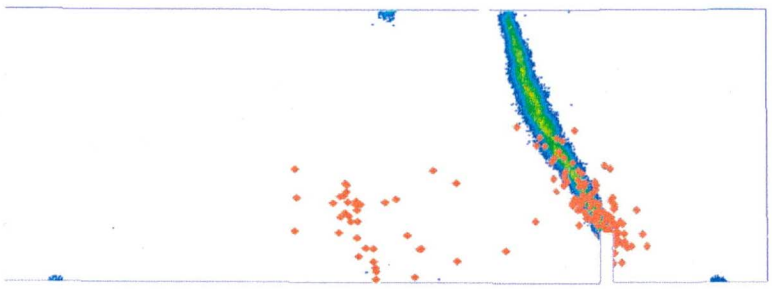

Figure 8: Failure in porous sandstone from three-point bending of a notched sample. Orange data is from acoustic emission measurements, black dots from a discrete element computation performed in the reference cited above, and the blue-green-yelow data is from the peridynamic model of a material with initial defects (pores).